The University of Tehran Press

Pollution

Print ISSN: 2383-451X
Online ISSN: 2383-4501

https://jpoll.ut.ac.ir/

Associations of Trace Gases and Meteorological Parameters and Particulate Matter with Ozone under Smog Conditions

Nishi Srivastava | **Apurba Tewari** | **Anik Das**

Department of Physics, Birla Institute of Technology, Mesra Ranchi 835215, India

Article Info

Article type:
Research Article

Article history:
Received: 4 October 2024
Revised: 18 February 2025
Accepted: 21 July 2025

Keywords:
Air Pollution
Smog
Ozone
VOC
Trace Gases

ABSTRACT

This work investigated the connection between O_3 and other pollutants and meteorological conditions during a smog episode in Delhi. Ozone concentrations varied from site to site (150~269µg/m^3). A significant negative correlation has been observed between O_3 and its precursor gases. Wind speed showed a positive correlation, but high wind usually dilutes the pollutant concentrations. Thus, a positive correlation with wind speed represents ozone transport from other locations to observational sites. The high ratio of $PM_{2.5}$ to PM10 indicates a predominance of human involvement. Toluene and benzene ratios(T/B) are estimated to understand the nature of emission sources and the lifetime of pollution. The analysis of the benzene and toluene fractions indicates anthropogenic air masses' dominance. Very high T/B values at several sites indicated that benzene was emitted from vehicular emission while toluene was from point sources. Ozone formation potential analysis showed that toluene and p-xylene are the prime contributors to ozone.

Cite this article: Srivastava, N., Tewari, A., & Das, A. (2025). Associations of Trace Gases and Meteorological Parameters and Particulate Matter with Ozone under Smog Conditions. *Pollution*, 11(3), 758-780.
https://doi.org/10.22059/poll.2025.383221.2585

DOI: https://doi.org/10.22059/poll.2025.383221.2585

INTRODUCTION

With the increased encroachment on natural resources, an alarming degradation has been noticed, and air quality is one of them. In recent years, severe air pollution episodes have increased significantly worldwide, and similar trends are also observed in India. The air quality in the northern region of India is a serious issue throughout the year and gets severe in the wintertime (Kumar et al., 2011). For various reasons, the air quality of the national capital, Delhi, and the nearby area, i.e., the National Capital Region (NCR), is of prime concern. Geographical location and the meteorological conditions perceived during the winter over Delhi and NCR region cause severe pollution (WHO 2016).

In winter, a smog situation arises over this part, which leads to severe health implications (Rizwan et al., 2013). Smog, i.e., a mix of smoke and fog, is air pollution that impairs visibility. Smog is a mixture of pollutants, with ground-level ozone as the prime component. Photochemical haze makes up most of the smog we encounter these days. When sunlight combines with nitrogen oxides (NOx) and at least one volatile organic compound (VOC) in the atmosphere, photochemical smog is created. Metro-cities are observing a tremendous increase in the various pollutants dangerous to human health and the ecosystem. During the last few decades, secondary and primary pollutant concentrations have increased significantly (Notario et al.,

*Corresponding Author Email: *nishi.bhu@gmail.com*
nsrivastava@bitmesra.ac.in

2012). Various cities around the globe are monitoring the enhanced concentration of VOCs, ozone, NOx, benzene, and several other trace pollutants, which are the root cause of several cardiovascular diseases and are also harmful to the flora-fauna (Fishman et al., 2010).

Among all the pollutants, ozone has peculiar characteristics, such as its usefulness or severity for humans, and the ecosystem depends on its altitude. Ozone in the lower atmosphere, i.e., troposphere, causes severe health issues related to respiration (Krupa and Manning, 1988). It is not a primary pollutant but formed as a secondary pollutant by the reaction of NOx and VOCs in the presence of solar radiation. Industrial and vehicular emissions, gasoline vapour, and other chemical exhausts from the industries are prime emitters of NOx in urban areas (Akther et al., 2023). Paints, gasoline, and various cleaning solvents emit VOCs (McDonald et al., 2018). Swift economic development in India has extraordinarily expanded the outflow of these ozone precursors (Duncan et al., 2016). The ozone generation from NOx and VOCs evolves complex photochemistry and depends on the emission rate of these pollutants (Seinfeld and Pandis, 2006; Alam et al., 2024). Figure 1 gives a schematic diagram of tropospheric ozone production (Zhang et al., 2019).

VOCs are one of the omnipresent groups of organic constituents in nature (Calfapietra et al., 2013; Saeedi et al., 2024). Benzene, toluene, and xylene are prime VOCs present in the atmosphere (Feng et al., 2019). These pollutants exhibit cardiovascular, respiratory, neurological, carcinogenic, and irritant effects (Halios et al., 2022). These contaminants cause numerous cardiovascular, pulmonary, neurological, carcinogenic, and irritating effects (Alghamdi et al., 2014). These compounds also participate in many photochemical reactions in the presence of sunlight and hydroxyl, producing ozone (Ho et al., 2004; Khoder, 2007; Salvador et al., 2022). The photochemical reactivity is measured by Maximum Incremental Reactivity (MIR), which evaluates the fraction of ozone produced from a fraction of a VOC. Ozone production fluctuates with environmental factors, but on average, substances with high MIR values typically produce more ozone than those with lower MIR values. Ozone forming capacity of different VOCs, especially benzene, toluene, and xylene, is known as Ozone Formation Potential (OFP) (Wang et al. 2016). OFP is a parameter defined in terms of MIR to describe individual VOCs' role in forming tropospheric ozone (Hajizadeh et al. 2018). The following expression used to estimate OFP:

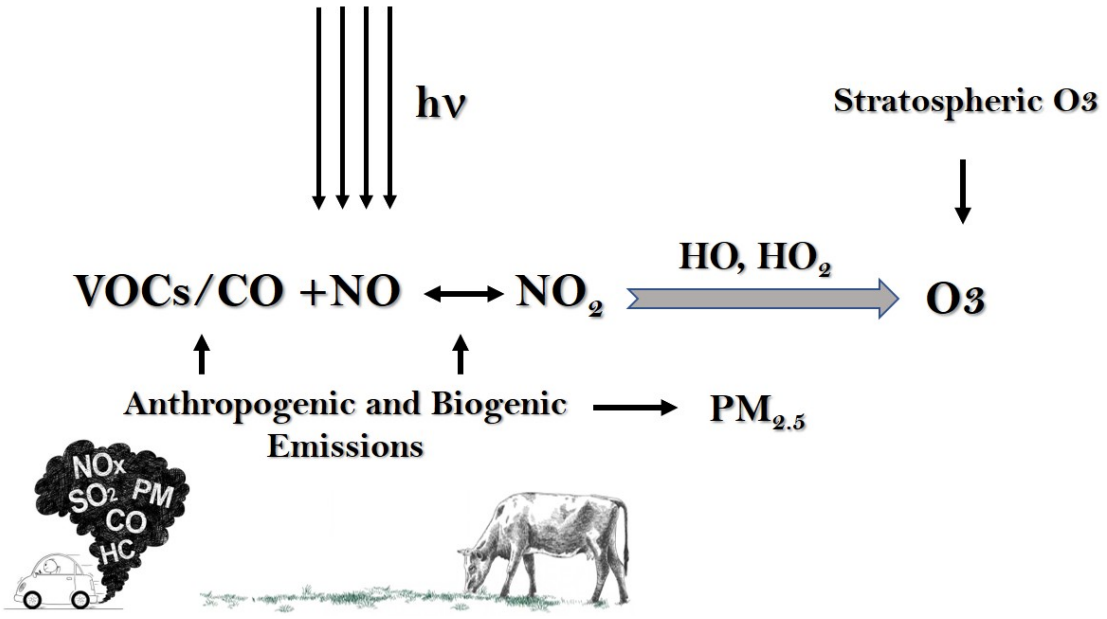

Fig. 1. Schematic diagram of the formation of Tropospheric Ozone

$$OFP_i = C_{VOC_i} \times MIR_i$$

where OFP_i, C_{VOC_i} (concentration), and MIR_i parameters are for a specific VOC.

To know the nature of the sources of emission of the VOCs, the toluene-to-benzene ratio (T/B) is useful and quantifies their role in ozone formation (Li *et al.*, 2021). The T/B ratio provides information regarding the distance between the sampling site and vehicular emissions, primarily in the urban areas dominated by vehicular emissions (Li et al., 2021).

Besides VOCs, particulate matter (PM) is another prime air pollutant in urban ambient air, which can moderate ozone production. Researchers have explored the relationship between ozone and PM and reported a non-linear relationship between these (Claire et al., 2019). Studies in various parts of the world showed that decreased PM is responsible for increased ozone concentration (Zhang et al., 2019; Li et al., 2019). Decreased aerosol concentration increases atmospheric visibility, and thus, surface-reaching solar radiation intensity increases, favouring ozone formation. At the same time, PM may act as a surface for various atmospheric reactions, leading to ozone formation (Zhang et al., 2019; Petrus et al., 2024).

In the present study, we investigated a smog episode over Delhi, which is a serious concern every winter. The role of trace gases in association with meteorological conditions in ozone formation during smog conditions is less explored. Thus, in the present work, we have performed a detailed analysis of the connection between O_3, its precursors (NO_x), trace gases (CO, benzene, toluene, p-xylene along with PM), and also the influence of meteorological conditions during a smog episode. These parameters have potential direct or indirect implications during severe smog conditions in Delhi; thus, it is essential to study these. The indicators T/B and OFP are also investigated to understand the nature of emissions and ozone formation processes. This manuscript is arranged in the following manner: the materials and methods, results and discussions, and finally, the conclusion.

MATERIALS & METHODS

Study site

This study was carried out in Delhi, the capital of India, which suffers from severe air pollution during the winter due to the combined effect of adverse atmospheric situations, high air pollutant concentrations, and smog. Delhi is geographically located between the latitudes of 28.24 °N to 28.53 °N and the longitudes of 76.50 °E to 77.20 °E (Hama et al., 2020). The study site is shown in Figure. 2. Delhi, with more than 11 million population, is listed as one of the most polluted cities of the world (Chandramouli and General, 2011; Jain et al., 2020). In India, Delhi has the highest number of registered automobiles. In 2011, there were roughly 6.93 million automobiles on Delhi's roadways, which is predicted to rise to 25.6 million by 2030 (Kumar et al., 2011). Thus, massive vehicular exhaust is released into the air.

Data used

Ambient air pollutant concentration and meteorological data were collected from the Real Time Ambient Air Quality data portal of the Delhi Pollution Control Committee (DPCC) for seven available locations (https://www.dpcc.delhigovt.nic.in/). These locations are RK Puram, Mandir Marg, Punjabi Bagh, Major Dhyan Chand National Stadium, Jawaharlal Nehru Stadium, Dr. Karni Singh Shooting Range, and Anand Vihar, which falls under residential, commercial, and industrial monitoring sites. The locations of the study sites are shown in Figure. 2. A brief description of monitoring locations with their station type and code is provided in Table 1. From

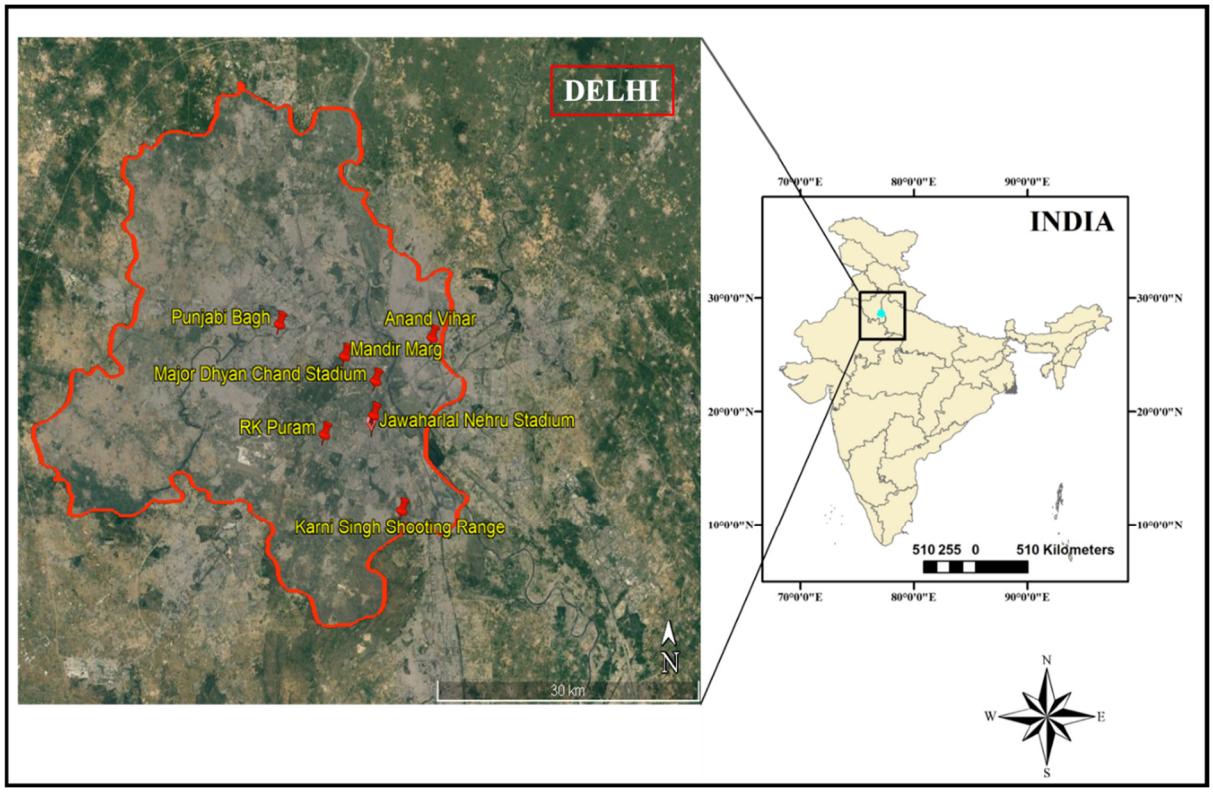

Fig. 2. Location of the study area

Table 1. Brief description of monitoring sites operated by DPCC (Delhi Pollution Control Committee)

Monitoring station	Site code	Type of site
RK Puram	RKP	Residential
Mandir Marg	MM	Residential & Commercial
Punjabi Bagh	PB	Residential, Industrial & Commercial
Major Dhyan Chand National Stadium	MDCS	Residential
Jawaharlal Nehru Stadium	JNS	Residential
Dr Karni Singh Shooting Range	KSR	Residential
Anand Vihar	AV	Residential, Industrial & Commercial

here on, the station codes are used for discussion. Pollutants and meteorological parameters are monitored at the Continuous Ambient Air Quality Monitoring Station (CAAQMS) (https://environment.delhi.gov.in) by DPCC. Along with the CAAQMS, DPCC also uses conventional technologies, Differential Optical Absorption Spectroscopy technique for gaseous pollutants measurement and the β-attenuation based principle for particulate matter sampling. The details of measurement techniques can be found on the site: https://environment.delhi.gov.in/.

Data Analysis

Ammonia, Benzene, Carbon Monoxide, Nitrogen Dioxide, Nitrogen Oxide, Oxides of Nitrogen, Ozone, p-Xylene, Sulphur Dioxide, Toluene, and Particulate Matter (<10µm and <2.5 µm) concentration data were collected for all the sites from DPCC data portal. The measurement units for all the pollutants are $\mu g/m^3$ except for CO, for which the measurement unit is mg/m^3. The meteorological parameters used in the present study are ambient temperature, barometric pressure, relative humidity, solar radiation, vertical wind speed, horizontal wind speed, and wind direction. The study was performed from 10 November 2017 to 19 January 2018, when

severe smog conditions persisted over the study region. During data filtering, dates that were missing from the datasets for contaminants or meteorological conditions were removed from the analysis. Following filtering, the hourly dataset was used to derive the diurnal averaged dataset and the daily mean dataset for the concentration of contaminants and meteorological parameters. For further analysis, these daily averaged datasets were used. The details of statistical parameters (i.e., minimum, maximum, and mean) of all the pollutants for November, December, and January are provided in Table 2 for each site. Ozone concentration was observed in a wide range over all the stations. During smog, sometimes the maximum ozone concentration values were more than 100 μg m^{-3}, though the averaged maximum values were mostly below near to 100 μg m^{-3}. The particulate matter concentrations ($PM_{2.5}$ and PM_{10}) over all the sites were severely high. The maximum concentration at each site showed that particulate matter (PM_{10}) concentrations sometimes shot more than 1200 μg m^{-3} and $PM_{2.5}$ more than 500 μg m^{-3}. The concentration of NOx, the prime precursor gas for ozone, was significantly higher at all the sites and sometimes reported more than 1000 μg m^{-3}. Detailed information regarding each pollutant is provided in Table 2.

RESULTS AND DISCUSSION

Diurnal Variation of Pollutants

First, we observed the diurnal variation of ozone and other precursor gases, i.e., NOx, VOCs (Benzene, Toluene, and p-Xylene), particulate pollutants (PM_{10}, $PM_{2.5}$), ammonia, and CO concentration in the ambient air for all the sites RKP, MM, PB, MDCS, JNS, KSR, and AV, respectively (Figure 3). Ozone concentration showed a low during the late evening to early morning and a peak in the afternoon over all the sites except the AV site. At the AV site, a random variation of ozone was observed. The highest ozone concentration was noticed over the RKP, JNS, and KSR residential sites, reaching about 100 μg/m^3. Over sites PB and MDCS, it was about 80μg/m^3, while over the other two locations (i.e., MM and AV) lowest ozone concentration was noticed (~45μg/m^3). Ozone concentration increases about 8-9 AM when solar radiation is sufficient for the start of photochemical reactions. The peak concentration was observed in the late afternoon ~3-4 PM, after which it started decreasing to the lowest in the evening in the decrease/absence of solar radiation. Oxides of nitrogen, CO, and VOCs are prime compounds in photochemical reactions for ozone generation and solar radiation. With the start of ozone generation, a decrease was noticed in NOx, CO, and VOCs (Toluene, Benzene, and p-Xylene) concentrations. The reduction in these reactants is observed in the same duration (after sunrise ~8 AM to sunset ~6 PM) in which an increase in the ozone concentration was observed. The highest concentration of NOx varied in the range of ~600-250 μg/m^3 from one site to another. After the start of photochemical reactions, a substantial decrease in NOx concentration could be noticed, reaching about 100 μg/m^3 or below. The maximum CO concentration varied from 5-10 μg/m^3 from one station to another while reducing to ~1 μg/m^3 during the peak photochemical reactions. Maximum benzene concentration ranged between 2.5-10 μg/m^{-3} except for MDCS and KSR sites. For these two sites, benzene concentration was very low compared to others, ranging between ~0.2-1 μg/m^3. The highest toluene concentration was observed at the MDCS site (~50 μg/m^3) and the lowest over the KSR site (~8 μg/m^3). Over other sites, toluene concentration varied between ~20-30 μg/m^3. Another VOC important in the generation of ozone is p-xylene. The maximum concentration of p-xylene varied from 10-16 μg/m^3 over most of the sites, except for the MDCS and KSR sites, which were about ~1.5 μg/m^3.

We have also studied the variation of ammonia in the ambient environment at study sites. As such, ammonia does not contribute to ozone formation, but in the aqueous form, ammonia

Table 2. Monthly mean concentrations (max-min) of ambient air pollutants at different locations in Delhi, India (November 2017-January 2018)

Location	Month	PM_{10} ($\mu g/m^3$)	$PM_{2.5}$ ($\mu g/m^3$)	NO_x ($\mu g/m^3$)	CO (mg/m^3)	Benzene ($\mu g/m^3$)	Toluene ($\mu g/m^3$)	Ozone ($\mu g/m^3$)	Ammonia ($\mu g/m^3$)	P-xylene ($\mu g/m^3$)
RKP	November	376.4 (724-169)	218.7 (392-63)	259.2 (1292.3-41.1)	2.8 (11.8-0.6)	8.6 (21-2.5)	25.6 (52.9-10.7)	28.8 (109.8-5.1)	43.3 (72.0-17.9)	11.8 (39.5-1.0)
	December	376.2 (958- 77)	222.8 (495-45)	314.0 (1443.9-34.9)	3.7 (13.1-0.2)	9.0 (18.3-2.1)	26.8 (49.7-7.5)	25.1 (138.4-0.4)	42.8 (72.1-23.0)	12.3 (36.5-0.3)
	January	402.5 (1135-128)	224.6 (672-64)	250.5 (1354.1-16.7)	2.6 (13.8-0.1)	5.3 (18.8-0.5)	14.1 (44.7-1.3)	31.6 (143.8-0.2)	40.4 (134.8-1.6)	5.2 (30.7-0.2)
MM	November	278.8 (564-79)	189.8 (426-62)	90.4 (277.8-33.3)	1.8 (7.2-0.2)	2.8 (10.3-0.9)	11.7 (52.8-4.4)	20.5 (42-9)	22.0 (32.5-14.1)	3.3 (14.0-0.3)
	December	322.1 (687-64)	209.8 (481-25)	196.7 (784.9-41)	3.3 (14.9-0.2)	4.0 (14.4-1)	22.7 (89.7-4.4)	20.1 (189.9-1.1)	29.1 (66.2-13.6)	7.2 (31.1-0.4)
	January	374.3 (815-113)	249.8 (550-42)	163.6 (637.7-37.7)	4.0 (12.5-0.1)	3.7 (10.2-0.9)	15.4 (58.6-3)	41 (269.8-0.2)	31.5 (53.5-17.3)	5.3 (18.0-0.3)
PB	November	351 (733-113)	235.7 (471-58)	139.0 (605.4-39.7)	2.1 (6.7-0.3)	2.7 (63.9-0.3)	7.9 (85.4-0.9)	35.7 (89.2-0.3)	54.1 (78.4-28.6)	2.1 (14.2-0.1)
	December	391.6 (1018-78)	243.6 (613-48)	223.3 (1093.5-15.2)	3.0 (17.1-0.6)	4.5 (40.2-0.4)	17.6 (87.7-0.9)	44.1 (147.3-4.7)	69.9 (272.0-23.3)	5.8 (50.3-0.1)
	January	447.3 (1563-127)	276.6 (559-47)	201 (933.9-3.6)	3.1 (11.8-0.4)	3.1 (22.9-0.5)	10.7 (74.5-1.2)	40.6 (135.9-0.2)	66.5 (113.1-3.7)	3.8 (31.3-0.2)
MDCS	November	292.7 (622-157)	200.3 (433-77)	-	-	-	-	-	-	-
	December	412.9 (1019-85)	264.7 (759-50)	318.9 (1301-36.6)	3.2 (10.6-0.4)	0.7 (1.8-0.1)	46.1 (203-0.6)	19.3 (141.7-0.1)	40 (74.9-17.5)	1.3 (3.1-0.1)
	January	444.8 (879-117)	271.5 (563-51)	261.2 (1514.2-30.4)	3.4 (9.6-0.2)	0.4 (2.03-0.1)	4.2 (12.7-1.4)	18.5 (123.6-0.6)	51.9 (76.0-4.40)	0.9 (2.20-0.3)
JNS	November	284.6 (448-138)	220.8 (410-20)	-	-	-	-	-	-	-
	December	355.5 (791-58)	301 (594-55)	407.8 (1653-33.5)	3.1 (10.9-0.1)	1.6 (4.6-0.3)	15.5 (38.7-2.4)	25.4 (169.9-0.1)	76.6 (125.5-36.1)	2.1 (7.7-0.1)
	January	479.1 (880-124)	146.8 (197-50)	329.4 (1684.7-34.6)	3.0 (13.1-0.1)	1.3 (4.1-0.2)	9.0 (30.4-1.5)	27.2 (167.6-0.3)	71.7 (99.7-30.4)	1.9 (105.0-0.1)
KSR	November	342.4 (578-171)	223.3 (412-79)	-	-	-	-	-	-	-
	December	411.1 (1273-116)	270.5 (807-55)	148.2 (505-27.8)	2.4 (9.3-0.5)	0.6 (2.7-0.1)	4.1 (20.4-0.4)	37.7 (175.6-0.1)	39.3 (75.3-11.5)	1.5 (7.1-0.1)
	January	446.8 (975-149)	285.2 (624-68)	105.7 (396-21.3)	2.3 (7-0.6)	0.5 (1.3-0.1)	-	40.0 (24.0-2)	51.1 (75.3-16.1)	0.7 (3.2-0.1)
AV	November	295.7 (348-180)	235.4 (565-62)	265.1 (1226.7-51.3)	2.8 (9-0.1)	5.3 (14.8-1.2)	17.6 (93-3.7)	27.0 (163.6-8.9)	72.6 (156.4-34.7)	3.7 (23.2-0.6)
	December	578.0 (1175-57)	309.1 (725-55)	487.6 (1675-63.1)	3.7 (13.6-0.1)	8.5 (40.1-1.5)	20.8 (128.4-4.1)	28.2 (104-11.2)	107.2 (233.4-20.8)	8.6 (45.7-0.5)
	January	540.4 (1191-167)	315.5 (754-49)	433.0 (1633-20.8)	4.7 (86.2-0.1)	8.9 (23.3-0.7)	20.7 (98.2-4.6)	23.5 (67.3-3.8)	90.4 (218.2-6.6)	7.6 (44.0-0.7)

Dash (-) denotes the unavailability of data for that particular pollutant.

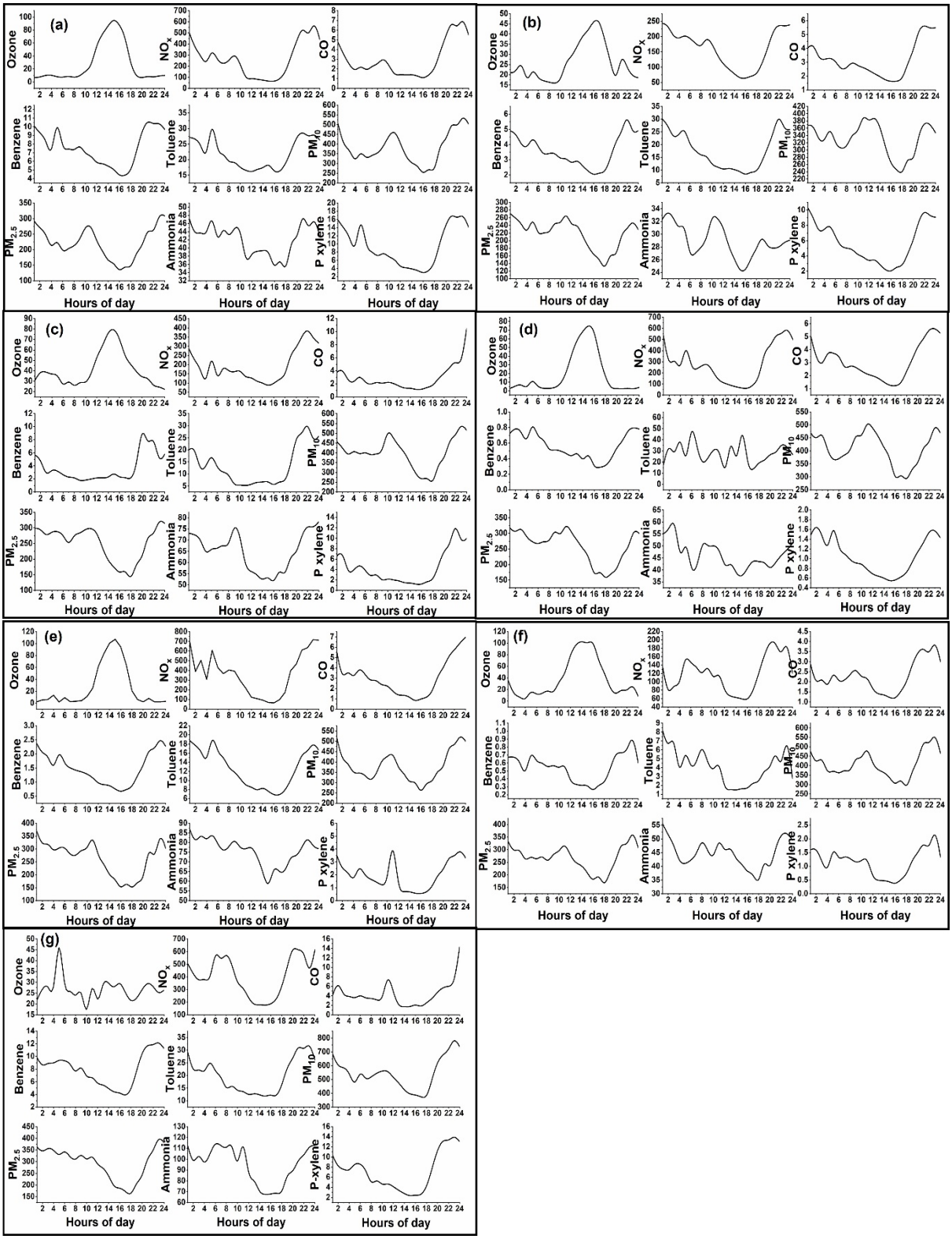

Fig. 3. Diurnal Variation of air pollutants at (a) RKP, (b) MM, (c) PB, (d) MDCS (Units: µg/m^3, for CO: mg/m^3), (e) JNS, (f) KSR, and (g) AV

reacts with ozone and gets oxidized. Ammonia can indirectly contribute to ozone generation as it contributes to nitrogen generation in the environment. Ambient ammonia is reported to contribute to $PM_{2.5}$ concentration by forming inorganic aerosols (Schiferl et al., 2014). Randomness is observed in the variation of the ammonia, though a slightly lower concentration was observed during the time of the highest ozone concentration. The maximum concentration of ammonia varied between 32-85 $\mu g/m^3$ range except at the AV site, where it was about 110 $\mu g/m^3$.

Variability of the $PM_{2.5}/PM_{10}$ Ratio

Next, we studied the variation in particulate matter ($PM_{2.5}/PM_{10}$) ratio. It is significant to study the $PM_{2.5}/PM_{10}$ ratio as it shows the relative abundance of coarser particles to finer particles, essential in ozone-producing chemical reactions. A lower ratio, i.e., the more significant amount of coarser particles, is usually associated with a higher potential for ozone production because of the increased surface area for heterogeneous chemical reactions.

The particulate matter indirectly alters the ozone concentration by acting as a sink for compounds contributing to ozone generation. Particulate matter diurnal variation (PM_{10} and $PM_{2.5}$) shows the two peak variations corresponding to high traffic emissions (Figure 3). According to Li et al., 2004 most primary and secondary anthropogenic combustion products that comprise fine particles ($PM_{2.5}$) come from energy generation and traffic. Due to its smaller size, longer atmospheric duration, and more significant health concerns when compared to PM_{10}, $PM_{2.5}$ receives more attention (Dominici et al., 2014).

The $PM_{2.5}/PM_{10}$ ratio can provide important information about the particle origin, its formation process, and its effects on human health because fine and coarse particles perform different physic-chemical properties and come from various sources (Speranza et al., 2023; Blanco-Becerra et al., 2015). Smaller ratios show significant involvement of coarse particles, which may be attributed to natural causes, such as dust storms, while higher ratios of $PM_{2.5}/PM_{10}$ attribute particle pollution to anthropogenic sources (Sugimoto et al., 2016). This ratio shows features of particle pollution since different sources typically create finer and coarser particles. Without direct measurements, the ratio can be used to analyze historical $PM_{2.5}$ pollution and identify the underlying atmospheric processes. The variation of $PM_{2.5}/PM_{10}$ is shown in Figure 4.

The ratio of $PM_{2.5}$ to PM_{10} varies between 0.36 to ~0.91 overall sites. All sites show similar variation, with a high $PM_{2.5}/PM_{10}$ ratio in the morning and a decrease in the afternoon. The JNS site showed the highest ratio of other sites and was noticed between 0.7-0.9 in the morning. The lowest value of this ratio was detected at the AV site (~0.36) in the evening hours and the highest at JNS (~0.91) in the morning hours. The high value of the $PM_{2.5}$ to PM_{10} ratio is indicative of dominant anthropogenic contributions. In the wintertime, anthropogenic emission dominates owing to various factors, and a similar indication could also be observed in the particulate matter ratio. The result showed that JNS was the most polluted site concerning anthropogenic particulate matter emissions. This ratio for all the sites had lowered after noontime.

Details of the mean concentration of each pollutant over every site and their maximum and minimum concentration for each month (i.e., November 2017 to January 2018) are shown in Table 2. This provides us with the range of variation of each pollutant during the respective months at each site.

Correlation of Ozone with other pollutants

Estimating the correlation between ozone and its precursor gases is essential to quantify their role in ozone formation. Figure 5 depicts the correlation of ozone with other pollutants

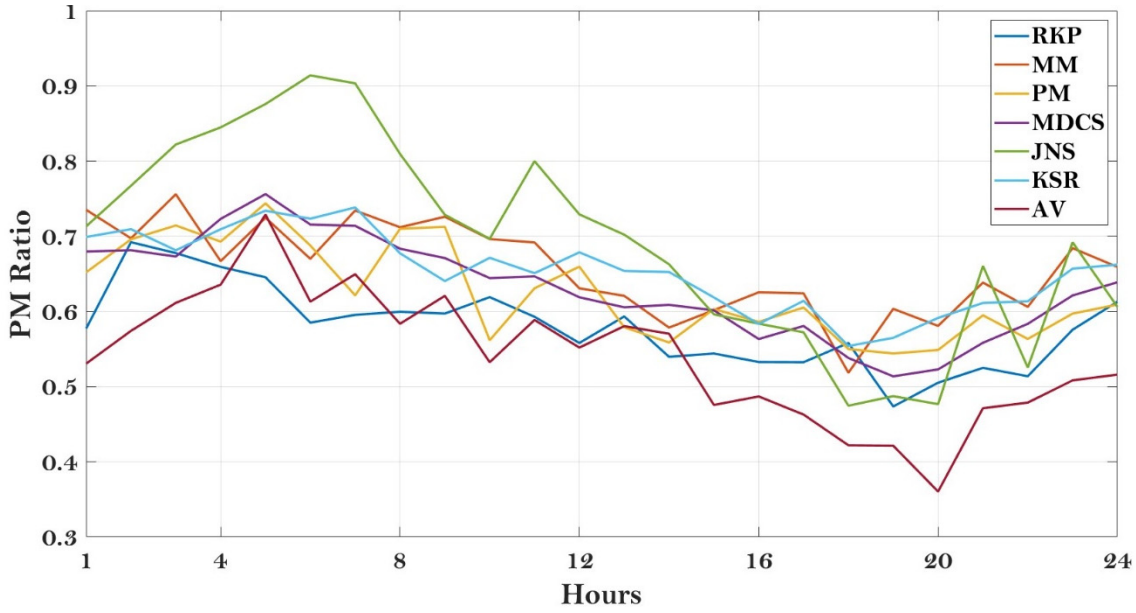

Fig. 4. $PM_{2.5}/PM_{10}$ ratio at all study sites

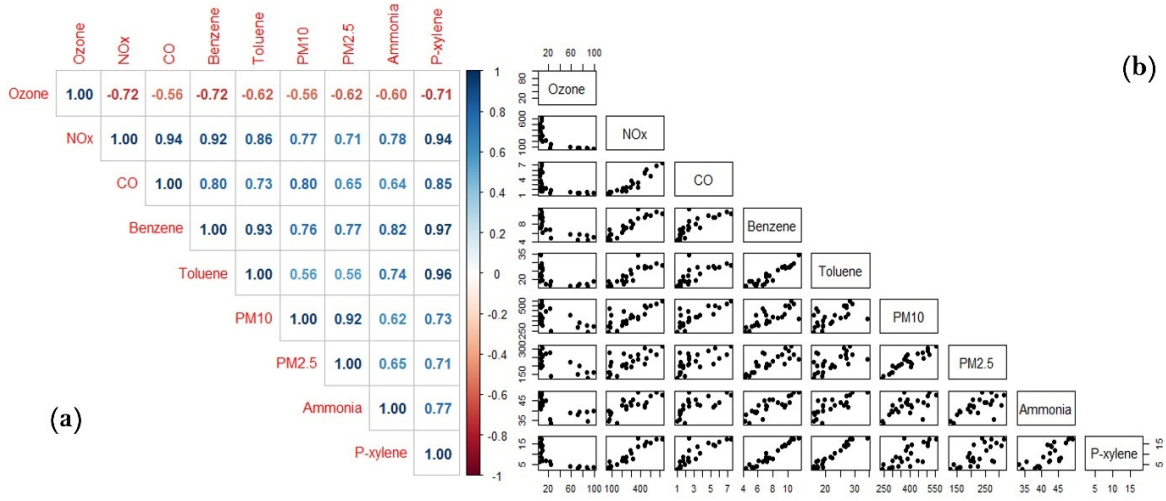

Fig. 5 Correlation matrix air pollutants at the RKP site

over the RKP site with the help of a correlation matrix. Simply glancing at the raw data would make it exceedingly difficult to see the connection between each variable. Correlation data can be suitably arranged using a correlation matrix. A correlation matrix provides an easily understandable representation of correlation values between the various parameters. The correlation matrix displays the correlation values, which quantify how closely each pair of variables is related linearly. Figure 5(a & b) provides the numerical values and pictorial representation of the correlation of ozone with various other precursor gases and pollutants for the RKP site. We can observe that ozone had a strong negative correlation with its precursor gases (i.e., NOx and CO) and VOCs (Benzene, Toluene, and p-Xylene), which act as catalysts in photochemical reactions. NOx is the prime constituent in the photochemical reaction for ozone formation; thus, a strong negative correlation was noticed between these. Table 3 provides details of correlation values between these pollutants for each station. A negative correlation

Table 3. Correlation matrix table showing Pearson's correlation coefficient (r) values

Location	Pollutants	Ozone	NO_x	CO	Benzene	Toluene	PM_{10}	$PM_{2.5}$	Ammonia	P-xylene
	Ozone	1								
	NO_x	-0.72	1							
	CO	-0.56	0.94	1						
RKP	Benzene	-0.72	0.92	0.80	1					
	Toluene	-0.62	0.86	0.73	0.93	1				
	PM_{10}	-0.56	0.77	0.80	0.76	0.56	1			
	$PM_{2.5}$	-0.62	0.71	0.65	0.77	0.56	0.92	1		
	Ammonia	-0.60	0.78	0.64	0.82	0.74	0.62	0.65	1	
	P-xylene	-0.71	0.94	0.85	0.97	0.96	0.73	0.71	0.77	1
	Ozone	1								
	NO_x	-0.77	1							
	CO	-0.53	0.86	1						
MM	Benzene	-0.61	0.91	0.93	1					
	Toluene	-0.57	0.92	0.86	0.96	1				
	PM_{10}	-0.31	0.47	0.43	0.49	0.40	1			
	$PM_{2.5}$	-0.48	0.63	0.41	0.52	0.49	0.90	1		
	Ammonia	-0.50	0.52	0.30	0.38	0.40	0.50	0.64	1	
	P-xylene	-0.60	0.94	0.91	0.96	0.99	0.44	0.53	0.43	1
	Ozone	1								
	NO_x	-0.57	1							
	CO	-0.55	0.75	1						
PB	Benzene	-0.34	0.75	0.61	1					
	Toluene	-0.52	0.88	0.79	0.90	1				
	PM_{10}	-0.64	0.54	0.59	0.31	0.48	1			
	$PM_{2.5}$	-0.66	0.40	0.49	0.15	0.38	0.90	1		
	Ammonia	-0.82	0.70	0.67	0.41	0.63	0.71	0.73	1	
	P-xylene	-0.58	0.89	0.83	0.85	0.97	0.57	0.45	0.68	1
	Ozone	1								
	NO_x	-0.69	1							
	CO	-0.64	0.98	1						
MDCS	Benzene	-0.05	-0.07	0.09	1					
	Toluene	-0.55	0.72	0.76	0.28	1				
	PM_{10}	-0.21	0.25	0.32	0.12	0.47	1			
	$PM_{2.5}$	-0.29	0.20	0.28	0.16	0.59	0.91	1		
	Ammonia	-0.46	0.42	0.45	0.56	-0.01	0.43	0.53	1	
	P-xylene	-0.69	0.83	0.84	0.93	0.39	0.32	0.42	0.62	1
	Ozone	1								
	NO_x	-0.80	1							
	CO	-0.70	0.97	1						
JNS	Benzene	-0.73	0.96	0.93	1					
	Toluene	-0.73	0.90	0.82	0.95	1				
	PM_{10}	-0.56	0.76	0.79	0.79	0.60	1			
	$PM_{2.5}$	-0.55	0.62	0.55	0.72	0.70	0.74	1		
	Ammonia	-0.72	0.70	0.60	0.72	0.74	0.57	0.75	1	
	P-xylene	-0.60	0.71	0.71	0.74	0.61	0.79	0.67	0.52	1

Table 3. Correlation matrix table showing Pearson's correlation coefficient (r) values

Location	Pollutants	Ozone	NO_x	CO	Benzene	Toluene	PM_{10}	$PM_{2.5}$	Ammonia	P-xylene
KSR	Ozone	1								
	NO_x	-0.61	1							
	CO	-0.61	0.91	1						
	Benzene	-0.71	0.81	0.86	1					
	Toluene	-0.59	0.54	0.61	0.80	1				
	PM_{10}	-0.40	0.59	0.78	0.77	0.59	1			
	$PM_{2.5}$	-0.47	0.49	0.65	0.79	0.67	0.94	1		
	Ammonia	-0.29	0.19	0.43	0.55	0.61	0.74	0.80	1	
	P-xylene	-0.69	0.80	0.86	0.97	0.81	0.76	0.77	0.57	1
AV	Ozone	1								
	NO_x	-0.07	1							
	CO	-0.01	0.48	1						
	Benzene	0.17	0.79	0.57	1					
	Toluene	0.21	0.67	0.45	0.92	1				
	PM_{10}	-0.15	0.66	0.68	0.88	0.78	1			
	$PM_{2.5}$	0.11	0.49	0.57	0.77	0.57	0.79	1		
	Ammonia	0.10	0.66	0.55	0.73	0.52	0.67	0.85	1	
	P-xylene	0.13	0.75	0.61	0.96	0.96	0.87	0.64	0.58	1

was seen at all the sites, and the values varied between -0.57 to -0.80, except at site AV. CO also contributes to ozone formation, and results showed a strong negative correlation between the concentrations of CO and ozone. The correlation values varied between -0.55 and -0.70 from one location to another; over the RKP site, it was reported as -0.56. The correlation values of VOCs over the RKP site varied as -0.72, -0.62, and -0.71 for benzene, toluene, and p-xylene, respectively. Over other sites also, a statistically significant correlation was observed between these VOCs and ozone concentration. A strong negative correlation between benzene and ozone was noticed at RKP, MM, JNS, and KSR sites, while correlation values were insignificant at PB and MDCS sites. Toluene concentration showed a strong negative correlation with respective ozone concentrations at all study sites; correlation values ranged between -0.52 and -0.73. P-xylene is also a monitored VOC that contributes to the generation of surface ozone. Over the RKP site, a high negative correlation was noticed, which was -0.71. Over other sites, a statistically significant negative correlation was also seen, and correlation values ranged from -0.58 to -0.71. Particulate matter does not contribute directly toward ozone formation but acts as a sink for the various reactants involved. At the same time, a higher $PM_{2.5}/PM_{10}$ ratio indicates reduced surface chemical reactions. The results showed a moderate to low negative correlation between particulate matter and ozone. Most of the time, these correlation values were statistically insignificant. Ammonia correlation with ozone also varied greatly from one station to another, and the correlation values were between -0.29 and -0.82.

In the previous results, we noticed that site AV behaved differently than other sites. Over this site, ozone variation also showed strange behaviour and association with different pollutants and meteorological parameters. The correlation values were low and statistically insignificant. The present result showed the non-dependence of the ozone on the well-known precursor gases. However, a detailed analysis is required at this site to reach any conclusive statement regarding behaviour.

Influence of Solar Radiation and Temperature

In addition to emissions from local sources, the ambient ozone level is significantly governed by local meteorological conditions. Among the several meteorological parameters, the role of solar radiation, temperature, and wind speed is vital in controlling the concentrations of pollutants in urban regions. We have investigated the dependence of surface ozone concentration on solar radiation and temperature over all the observational sites, and the results are shown in Figure 6 & 7. The ozone concentration values tend to increase with increasing solar radiation and temperature values, especially during the afternoon hours (10-18 hr) when the intensity of solar radiation is at its peak. As discussed, tropospheric ozone is formed by various precursor gases in the presence of solar radiation; thus, the presence of solar radiation is a crucial factor in ozone generation. In Figures 6 and 7, the subplots indicate the observational site in the following manner: (a) RKP, (b) MM, (c) PB, (d) MDCS, (e) JNS, (f) KSR, (g) AV, respectively. Results shown in Figure 6 indicate that ozone concentration increases a few after sunrise. An increase in surface ozone could be noticed at about 8-9 AM and reached its peak value a few hours later than the peak solar radiation, i.e., in the late afternoon hours. The peak concentration of ozone varied from one station to another, and maximum ozone concentration was noticed over the sites JNS and KSR. The ambient ozone concentration reached up to ~110 $\mu g/m^3$ at these sites. Except for the station AV, a relatively high ozone concentration (~80 μg/m3) was also noticed over other stations. Over site AV, diurnal ozone variation showed a different behaviour than other sites. Over this site, the ozone concentration does not significantly change with solar radiation. The ozone concentration was relatively low at this site and less modulated by solar radiation. The average concentration of ozone was about ~25 $\mu g/m^3$. The solar radiation intensity increases

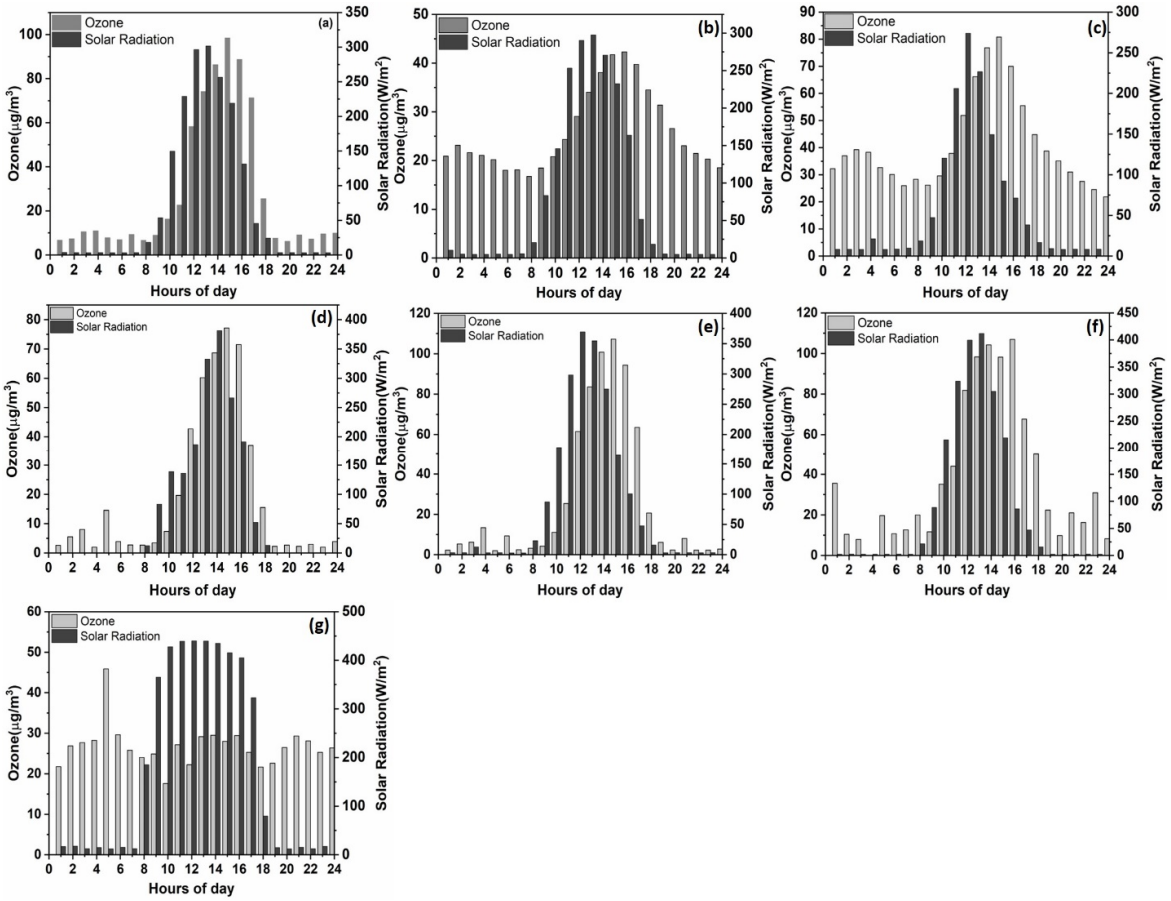

Fig. 6. Variation of ozone with solar radiation for (a) RKP, (b) MM, (c) PB, (d) MDCS, (e) JNS, (f) KSR, (g) AV

with sunrise, but ozone concentration did not change as it was noticed at other sites.

Next, we observed the changes in the ozone concentration corresponding to temperature change, though temperature changes align with radiation changes (Figure 7). The ozone concentration values tend to increase with increasing temperature values, especially during the afternoon hours (10-18 hr) when the intensity of solar radiation and corresponding air temperature is at its peak. In the lower temperature regimes (<10 ºC), ozone concentrations decrease rapidly with decreasing values of solar radiation intensity. Since the ozone photochemical production rate depends strongly on temperature (Figure 7), the highest O_3 concentrations were observed at air temperatures >15ºC. Solar intensity, which is directly related to air temperature, is necessary for ozone synthesis.

Role of Wind Speed Pollutants concentration moderation

We have also investigated wind speed's role in moderating the concentration of various air pollutants. The diurnal variation of various pollutants has been studied along with the diurnal variation of the wind (Figure 8 & 9). Figure 8 shows the ozone, CO, ammonia, and NOx variation with wind, while Figure 9 shows the variation of VOCs (Toluene, Benzene, and p-Xylene) with wind speed. The ozone concentration and wind speed showed a similar diurnal cycle, i.e., an increase in the value with sunrise and a decrease in the value with sunset. Though wind speed and ozone concentration varied similarly, it is difficult to state that they are interlinked, as ozone concentration changes with the solar diurnal cycle. Wind speed and

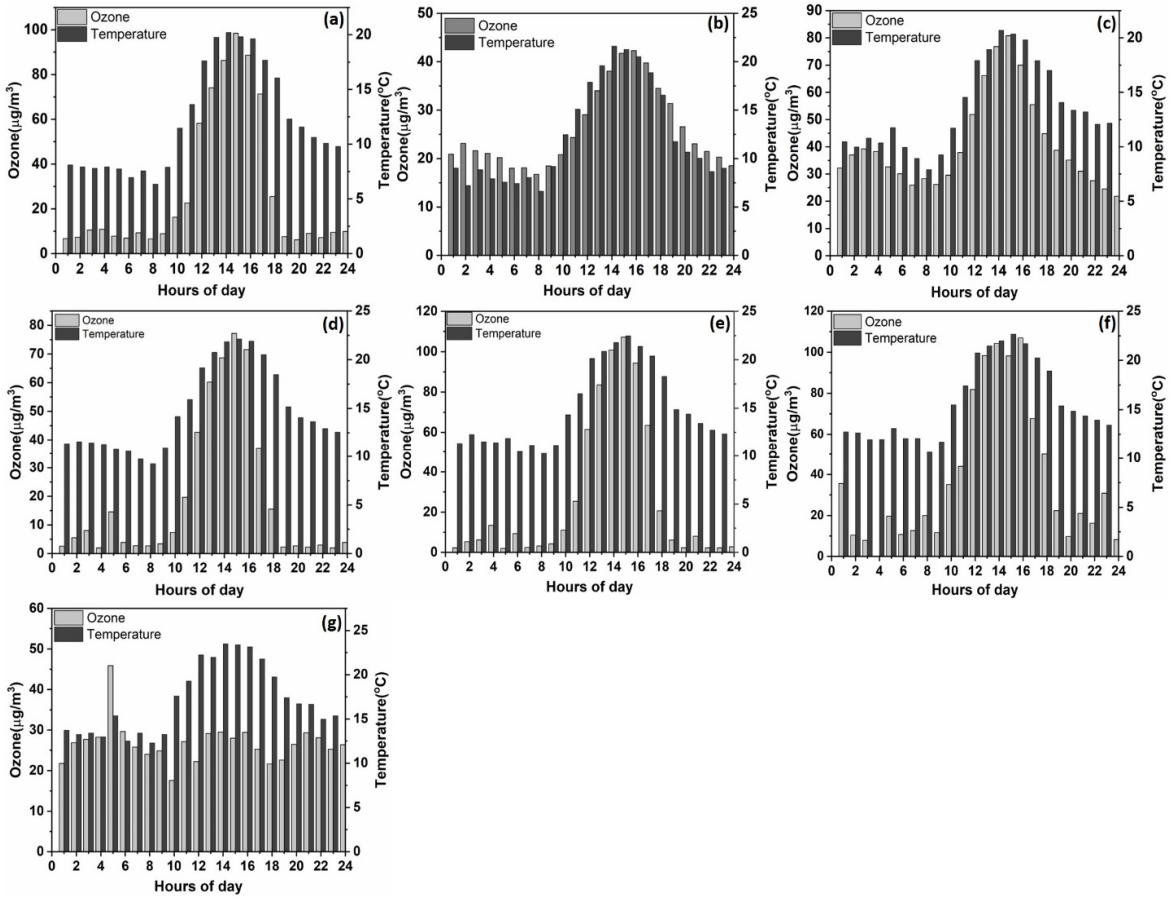

Fig. 7. Variation of ozone with temperature for (a) RKP, (b) MM, (c) PB, (d) MDCS, (e) JNS, (f) KSR, (g) AV

direction prominently contribute to diluting and transporting pollutants. Other than Ozone, the pollutants NOx, CO, benzene, toluene, and p-xylene showed opposite diurnal variation than wind speed, i.e., low daytime and high nighttime values. With the increase in solar insolation, the surface temperature increases, affecting the wind's strength over a location. These plots indicate that other than the chemical activities during the daytime, wind also contributes to the dilution of these pollutants by the effect of the dispersion of pollutants.

Toluene to Benzene ratio

The VOCs benzene and toluene play a role in ozone generation and control. Benzene and toluene, emitted into the atmosphere by various everyday anthropogenic activities, pose a significant risk to human health. The analysis of benzene and toluene fractions at study sites indicates the likely anthropogenic sources of the air masses sampled. The T/B ratio indicates emissions from traffic and non-traffic sources (Shi et al. 2015). Benzene and toluene are emitted in vehicular emissions, but benzene is frequently used to indicate vehicular emissions and toluene as emission from paint and related items and its industry (Miller et al., 2012; Liu et al., 2008). Lower ratio values represent vehicular emission dominance, while higher ratio values indicate the effect of industrial emission. Following the classification values from other researchers, we fixed the T/B ratio to be lower than three as indicative of vehicular emission and greater than three as non-vehicular emission (Ho et al., 2004; Miller et al., 2011).

To understand the vehicular/industrial emission pattern, we have also estimated the Toluene

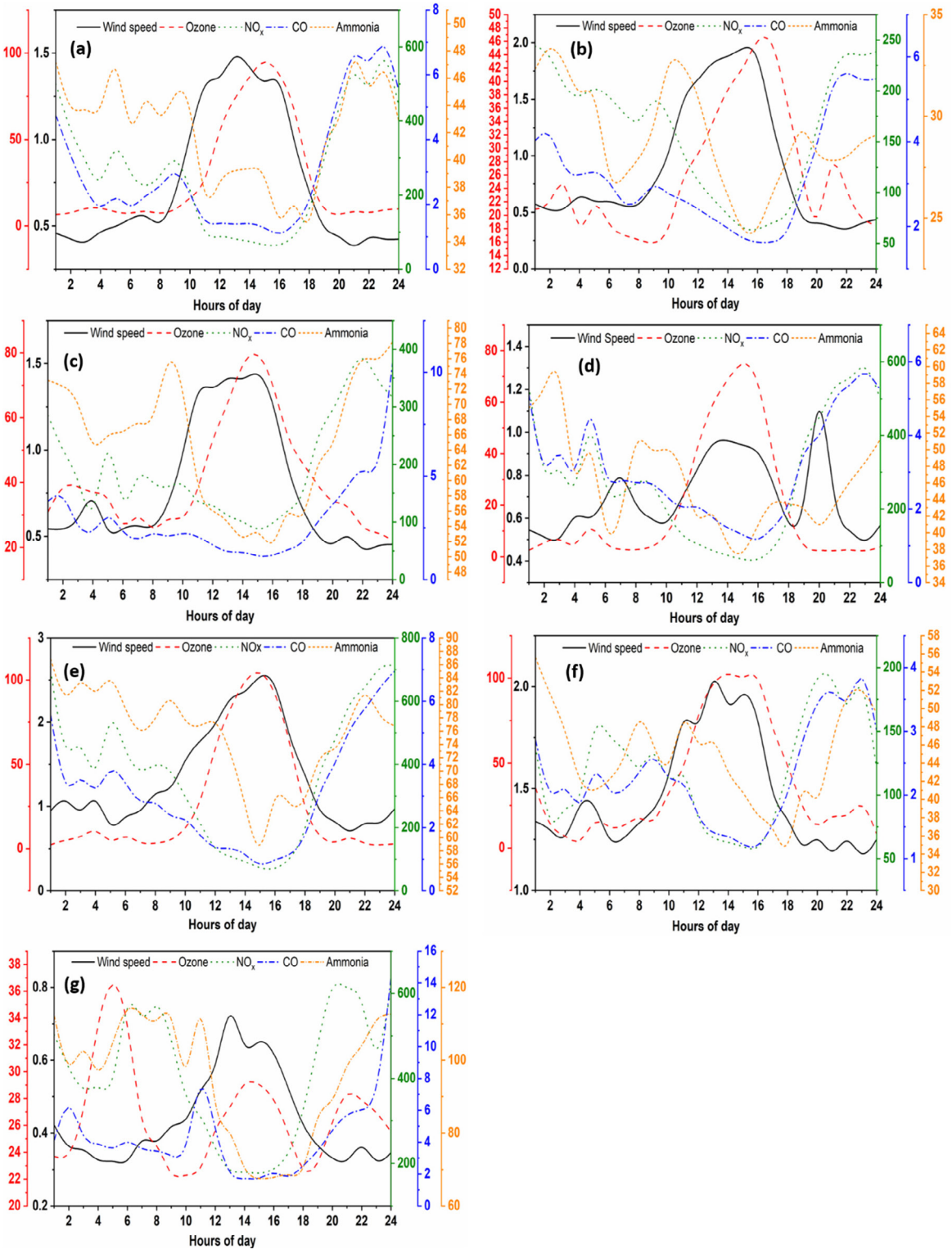

Fig. 8. Variation of ozone, NOx, CO and Ammonia with wind speed in (a) RKP, (b) MM, (c) PB, (d) MDCS, (e) JNS, (f) KSR, (g) AV.

to Benzene ratio for all study sites. The toluene-to-benzene ratio is frequently used to assess the air mass age due to the different reactivity of both with OH (Warneke et al., 2001). Researchers use the ratio between the VOCs (toluene to benzene, and (m + p)-xylene to ethylbenzene) to investigate the source origination and the photochemical age of the air mass at a particular

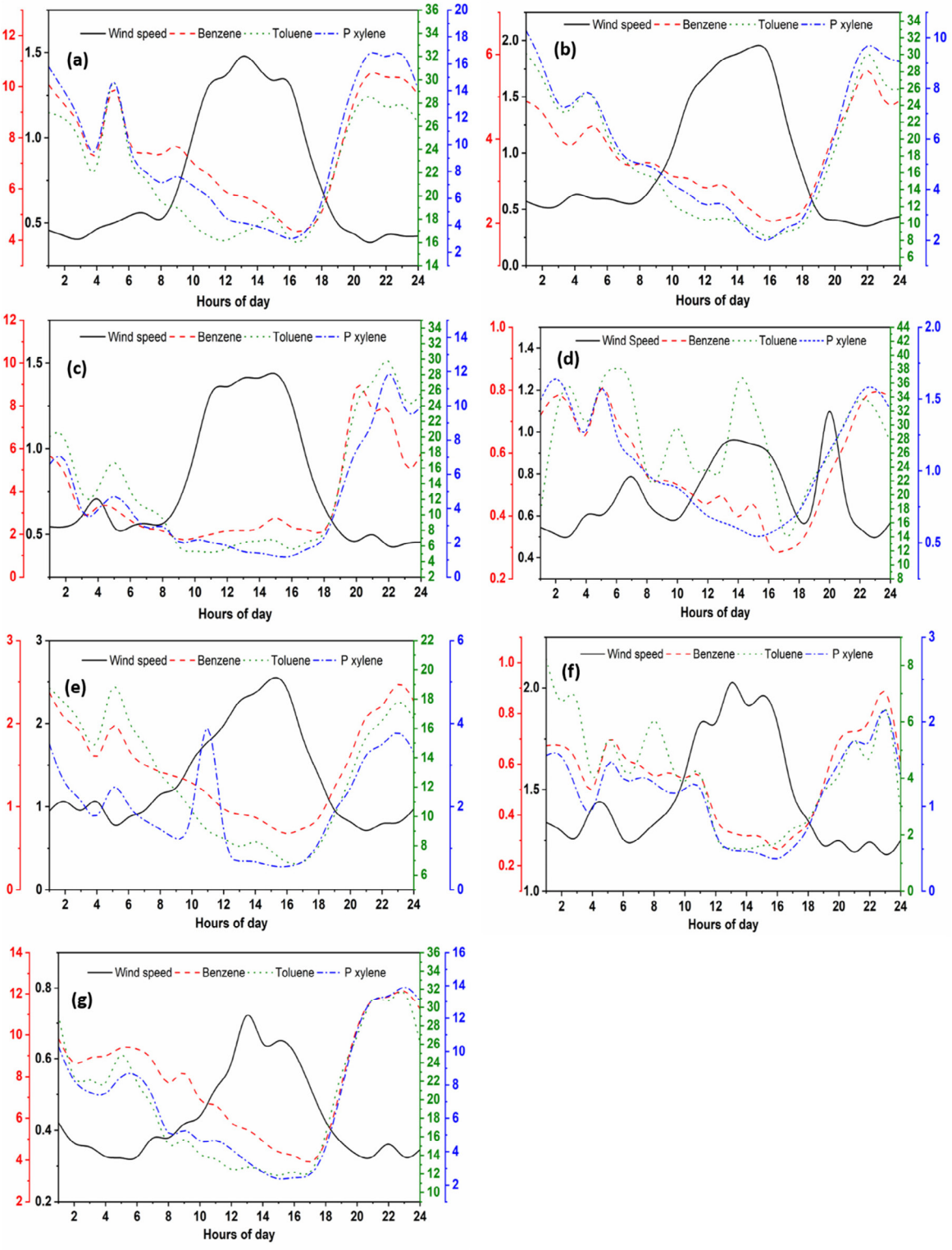

Fig. 9. Benzene, toluene and p-xylene concentrations in accordance with wind speed in (a) RKP, (b) MM, (c) PB, (d) MDCS, (e) JNS, (f) KSR, (g) AV.

location. The toluene to benzene ratio offers details on the traffic emission, while ($m + p$)-xylene to ethylbenzene ratio is used as an indicator of air of photochemical mass (Barletta et al., 2005; Liu et al., 2009). Research at various places showed that the T/B ratio values range from 1.5 to

Table 4. Statistical Parameters for Toluene to Benzene ratio over observational sites

Station Name	Mean T/B ratio	Maximum T/B ratio	Minimum T/B ratio	Standard Deviation	Correlation Coefficients
RKP	2.96	4.44	2.29	0.42	0.93
MM	4.62	7.89	2.85	1.03	0.96
PB	3.80	10.75	1.30	1.72	0.90
MDCS	11.71	23.18	3.60	4.70	0.49
JNS	9.34	33.49	3.39	5.19	0.95
KSR	7.06	19.30	2.28	4.00	0.80
AV	2.86	6.92	0.99	1.42	0.92

3.0, with variances probably caused by multiple vehicle types and fuel compositions in different geographic locations (Miller et al., 2011; Chiang et al., 1996; Gelencs´er et al., 1997). Reacting with OH radicals, toluene and benzene concentrations are lowered, with toluene having a rate constant of around five times greater than benzene (Gelencs´er et al., 1997). Thus, the lower T/B ratio indicates an aged air mass, i.e., vehicular emissions have travelled and deteriorated, while the high T/B ratios indicate new vehicular emissions.

The T/B ratios mean ranged from *2.86 to 11.71* at different sites in the present study, indicating different vehicular concentrations, industrial contributions, and distances from the monitoring site. With a rate constant of toluene that is around five times greater than benzene, the concentration of toluene and benzene is lowered by their reactivity with OH radicals. Very large values indicate the industrial contribution dominance in the total emission. Usually, a T/B ratio between 1.5-3.0 indicates vehicular emission, and a value higher than this confirms the influence of point sources of toluene. Thus, very high T/B ratio values indicate that benzene was emitted from vehicles and toluene was released from mobile and point sources, i.e., industries. Table 4 provides detailed T/B information, including the mean value, minimum value, maximum value, standard deviation, and correlation between toluene and benzene.

Along with the T/B ratio, we have also investigated the correlation between Benzene and Toluene; variations are shown in Figure 10 for each site. The highest correlations were observed at MM and KSR sites, followed by JNS. High correlation implying that these compounds had a common source of emission. Sites MDCS and RKP showed a low correlation of about 0.54 and 0.69. At the same time, the T/B ratio was quite large at these sites, indicating that the emission source for these pollutants is other than vehicular emission and emitted from different sources. At other sites, the correlation between these pollutants was moderately high, indicating the impact of emissions from vehicles and industries.

Ozone Formation Potential

Ozone formation potential is a quantity that has been frequently utilized to explain the contribution of individual VOCs in tropospheric ozone formation. OFP at the observational sites was evaluated with the help of the Maximum Incremental Reactivity technique, shown by equation (1). Documented MIR values for Benzene, Toluene, and p-xylene are 0.72, 4.00, and 5.84, respectively (https://ww2.arb.ca.gov/sites/default/files/2020-12/cp_reg_mir-tables.pdf). With the help of the above information, we estimated the OFP at all the sites. Figure 11 shows the variation of composite OFP for toluene, benzene, and p-xylene over all the sites. The total concentrations of OFP were found from ~20–225 μg/m^3.

Toluene and p-xylene significantly contributed to OFP concentration. However, among these pollutants over some sites, toluene contributed the maximum, and over others, the p-xylene contribution was higher than toluene. Toluene OFP values ranged between ~13.5-89.5 μg/m^{3,} and p-xylene OFP values varied between ~6-130 μg/m^3. Toluene showed the highest OFP

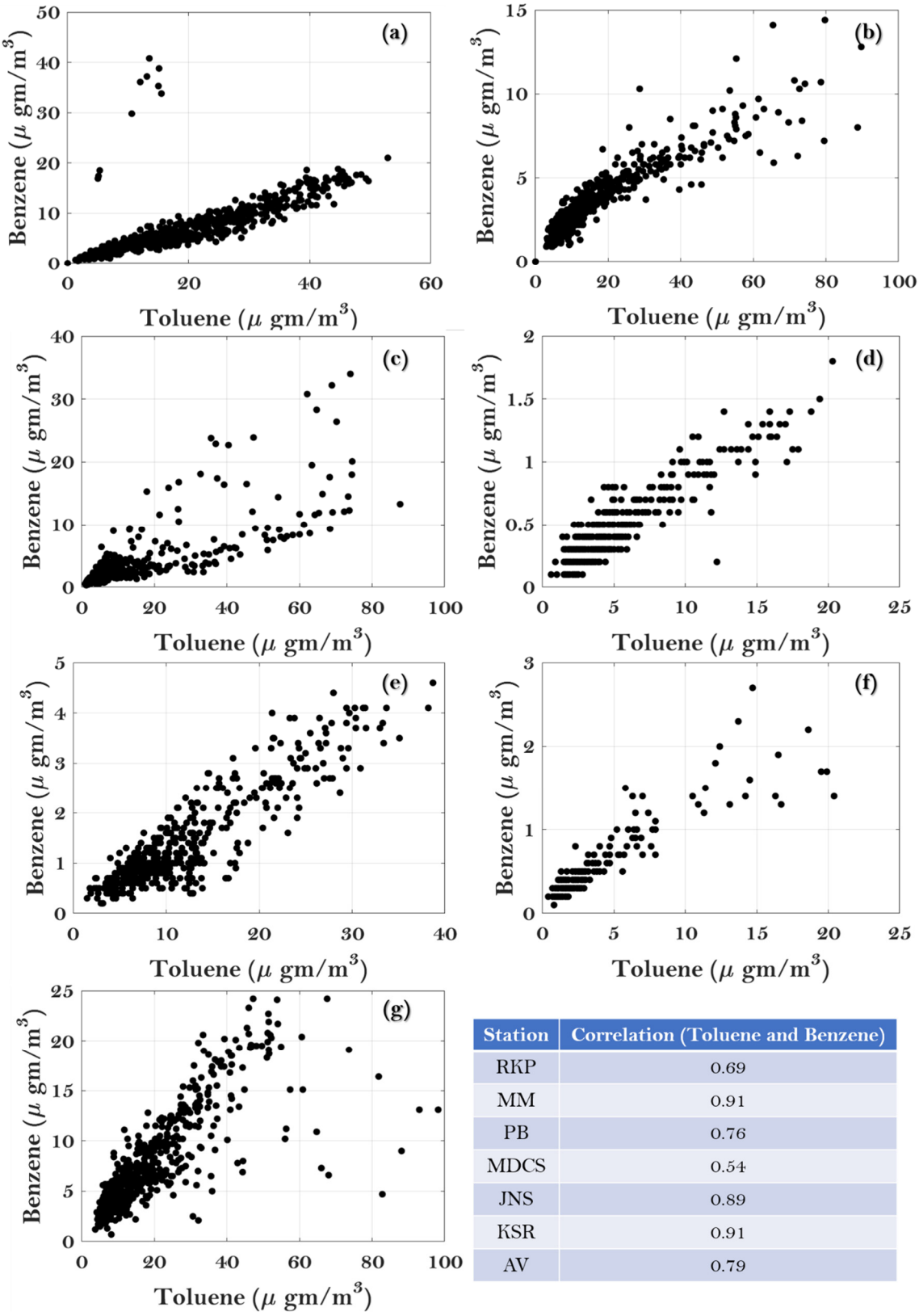

Station	Correlation (Toluene and Benzene)
RKP	0.69
MM	0.91
PB	0.76
MDCS	0.54
JNS	0.89
KSR	0.91
AV	0.79

Fig. 10 Relationships of toluene and benzene (a) RKP, (b) MM, (c) PB, (d) MDCS, (e) JNS, (f) KSR, (g) AV and their correlation.

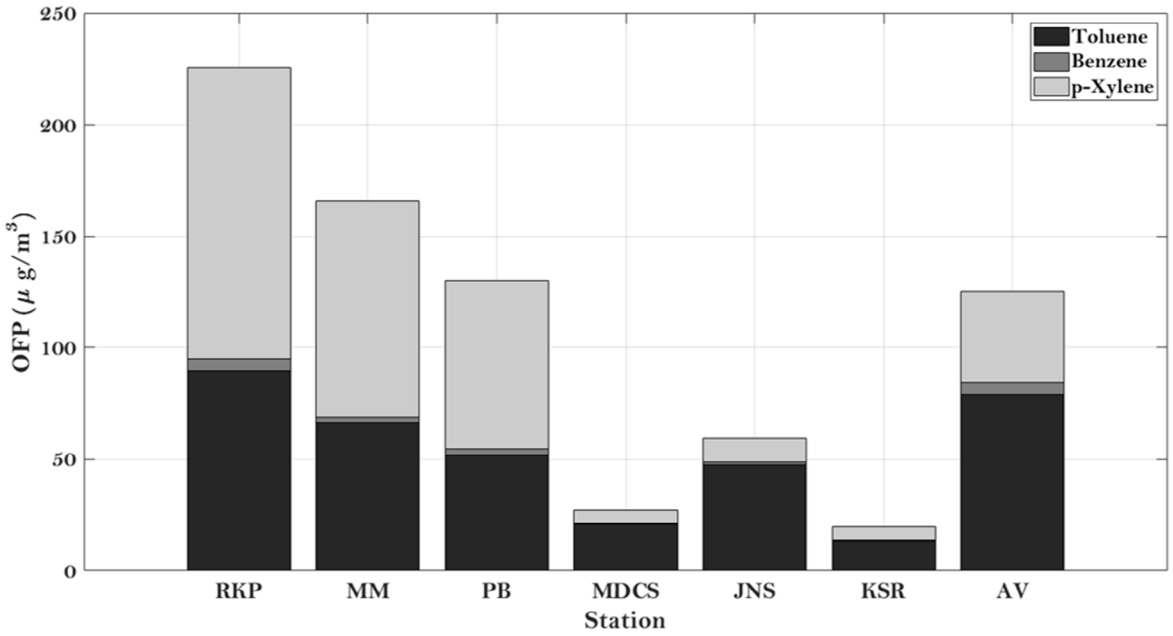

Fig. 11. Variation of composite OFP for toluene, benzene, and p-xylene over all the sites

values over MDCS, JNS, KSR, and AV sites, contributing between ~63%-90%. The study sites MDCS, JNS, and KSR are residential sites, while AV is Residential, Industrial & commercial. Over the residential sites (MDCS, JNS, and KSR), OFP value was significantly lower than Residential, Industrial & commercial sites. Over these sites, toluene was the prime contributor toward OFP, but similar was not seen at the RKP site, though it is also a residential site. Over other sites, i.e., at MM, PB, and RKP, p-Xylene was the main contributor to OFP, contributing ~58%. However, RKP is also reported as a residential site; the highest OFP value was seen over this site. In the total OFP, p-xylene contributed about ~58%, while toluene contributed ~40%. Benzene showed the lowest value of OFP among the three and was almost negligible compared to the other two pollutants OFPs over the MDCS, JNS, and KSR sites. Over other sites (i.e., AV, MM, PB, and RKP), benzene OFP values were low, but a notable value could be noticed.

The highest ozone concentration was observed at the PB and KSR sites, though OFP values over PB were moderate, while over KSR, the value of OFP was significantly low. The values of OFP were most significant over RKP, while the ozone concentration was moderate over RKP. The difference in the chemistry of each of the VOCs contributes towards the different impacts of VOCs on ozone formation.

CONCLUSION

This study investigates the role of various air pollutants, especially trace gases, and their association with ozone formation, along with various indicators of ozone formation during a smog episode. We also investigated the contribution of ozone formation capabilities of multiple pollutants, primarily VOCs. The prime findings of the work are:

• Most of the pollutants exhibited a clear diurnal cycle, where the ozone concentration increased during the daytime with a peak in the afternoon and subsequent decreases in the late evening. Few other pollutants (i.e., NOx, CO, benzene, toluene, and p-xylene) contributing to ozone formation showed exactly reversed diurnal cycle, i.e., increased value during nighttime,

while low values during the daytime. Particulate matter ($PM_{2.5}$ and PM_{10}) showed two peak variations corresponding to heavy traffic hours, and ammonia showed a random variation throughout the day.

• Though the ozone concentration was lower than its 8-hour allowed limit, it reached about 40 μg m^{-3}. Other pollutant concentrations were observed frequently above the ambient air's allowed concentration limits.

• The high ratio of $PM_{2.5}$ to PM_{10} indicates a predominance of human involvement. Due to several causes, anthropogenic emissions predominates in the winter, and the particulate matter ratio also shows this.

• The correlation matrix provides quantitative and visual information regarding the dependence of ozone on its precursor gases. A clear dependence of the ozone on NOx, CO, benzene, toluene, and p-xylene can be seen, and significant negative correlation values are observed.

• Solar radiation, high air temperature, and wind speed contributed to the high ozone concentration.

• The T/B ratios mean ranged from *2.86 to 11.71* at different sites, indicating different vehicular concentrations, industrial contributions, and distances from the monitoring site. Very high T/B ratio values indicate that benzene was emitted from vehicles and toluene was released from mobile and point sources, i.e., industries.

• Ozone formation potential is frequently used to find the contribution of various VOCs in tropospheric ozone formation. Toluene and p-xylene significantly contributed to OFP concentration. However, among these pollutants over some sites, toluene contributed the maximum, and over others, the p-xylene contribution was higher than toluene.

• The site AV behaved differently than all other sites; thus, further detailed analysis is essential to determine why it departed from expected behaviour.

ACKNOWLEDGEMENT

Authors thank DPCC (Delhi Pollution Control Committee) for the data.

GRANT SUPPORT DETAILS

The present research did not receive any financial support.

CONFLICT OF INTEREST

The authors declare that there is not any conflict of interests regarding the publication of this manuscript. In addition, the ethical issues, including plagiarism, informed consent, misconduct, data fabrication and/ or falsification, double publication and/or submission, and redundancy has been completely observed by the authors.

LIFE SCIENCE REPORTING

No life science threat was practiced in this research.

REFERENCE

Alam, J.M., Rappenglueck, B., Retama, A., & Rivera-Hernández, O. (2024). Investigating the

Complexities of VOC-Sources in Mexico City in the years 2016-2022. Atmosphere, 15, 179. https://doi.org/10.3390/atmos15020179

Alghamdi, M. A., Khoder, M., Abdelmaksoud, A. S., Harrison, R. M., Hussein, T., Lihavainen, H., ... & Hämeri, K. (2014). Seasonal and diurnal variations of BTEX and their potential for ozone formation in the urban background atmosphere of the coastal city Jeddah, Saudi Arabia. Air quality, atmosphere & health, 7, 467-480.

Akther, T., Rappenglück, B., Osibanjo, O., Retama, A., & Rivera-Hernández, O. (2023). Ozone precursors and boundary layer meteorology before and during a severe ozone episode in Mexico City. Chemosphere, 137978, DOI:10.1016/j.chemosphere.2023.13797

Blanco-Becerra, L. C., Gáfaro-Rojas, A. I., & Rojas-Roa, N. Y. (2015). Influence of the sweep effect on the PM2.5/PM10 ratio in the Kennedy area of Bogotá, Colombia, Colombia. Revista Facultad De Ingeniería Universidad De Antioquia, 76, 58–65. https://doi.org/10.17533/udea.redin.n76a07

Barletta, B., Meinardi, S., Rowland, F. S., Chan, C. Y., Wang, X., Zou, S., Chan,L. Y., & Blake, D. R. (2005). Volatile organic compounds in 43 Chinese cities. Atmospheric Environment, 39(32), 5979-5990. https://doi.org/10.1016/j.atmosenv.2005.06.029.

Calfapietra, C., Fares, S., Manes, F., Morani, A., Sgrigna, G., & Loreto, F. (2013). Role of Biogenic Volatile Organic Compounds (BVOC) emitted by urban trees on ozone concentration in cities: a review. Environ Pollut. 183, 71–80. doi: 10.1016/j.envpol.2013.03.012

Claire, E. B., Aaron, K., Udaysankar N., & Daniel, A. J. (2019). Relationships between Particulate Matter, Ozone, and Nitrogen Oxides during Urban Smoke Events in the Western US. Environmental Science & Technology, 53 (21), 12519-12528, DOI: 10.1021/acs.est.9b05241

Chandramouli, C., & General, R. (2011). Census of India 2011. Provisional Population Totals. New Delhi: Government of India, 409–413.

Chiang, P. C., Chiang, Y. C., Chang, E. E., & Chang, S. C. (1996). Characterizations of hazardous air pollutants emitted from motor vehicles. Toxicological and Environmental Chemistry, 56(1–4), 85–104. https://doi.org/10.1080/02772249609358352

Dominici, F., Greenstone, M., & Sunstein, C. R. (2014). Science and regulation. Particulate matter matters. Science. 344(6181):257-9. doi: 10.1126/science.1247348. PMID: 24744361, PMCID: PMC4206184.

Duncan, B. N., Lamsal, L. N., Thompson, A. M., Yoshida, Y., Lu, Z., Streets, D. G., Hurwitz, M. M., & Pickering, K. E. (2016). A space-based, high-resolution view of notable changes in urban NOx pollution around the world (2005–2014). Journal of Geophysical Research, 121(2), 976–996. https://doi.org/10.1002/2015JD024121

Feng, R., Wang, Q., Huang, Cc. Liang, J., Luo, K., Fan, Jr., & Zheng, Hj. (2019). Ethylene, xylene, toluene and hexane are major contributors of atmospheric ozone in Hangzhou, China, prior to the 2022 Asian Games. Environ Chem Lett 17, 1151–1160. https://doi.org/10.1007/s10311-018-00846-w

Fishman, J., Creilson, J.K., Parker, P.A., Ainsworth, E.A., Vining, G.G., Szarka, J., Booker, F.L., & Xu, X. (2010). An investigation of widespread ozone damage to the soybean crop in the upper Midwest determined from ground based and satellite measurements. Atmos. Environ. 44, 2248–2256. https://doi.org/10.1016/j.atmosenv.2010.01.015

Gelencs´er A., Siszler, K., & Hlavay, J. (1997). Toluene-benzene concentration ratio as a tool for characterizing the distance from vehicular emission sources. Environmental Science and Technology, 31(10), 2869– 2872. https://doi.org/10.1021/es970004c

Hama, S. M. L., Kumar, P., Harrison, R. M., Bloss, W. J., Khare, M., Mishra, S., Namdeo, A., Sokhi, R., Goodman, P., & Sharma, C. (2020). Four-year assessment of ambient particulate matter and trace gases in the Delhi-NCR region of India. Sustainable Cities and Society, 54, 102003. https://doi.org/10.1016/j.scs.2019.102003

Hajizadeh, Y., Mokhtari, M., Faraji, M., Mohammadi, A., Nemati, S., Ghanbari, R., ... & Miri, M. (2018). Trends of BTEX in the central urban area of Iran: A preliminary study of photochemical ozone pollution and health risk assessment. Atmospheric Pollution Research, 9(2), 220-229.

Halios, C. H., Landeg-Cox, C., Lowther, S. D., Middleton, A., Marczylo, T., & Dimitroulopoulou, S. (2022). Chemicals in European residences–Part I: A review of emissions, concentrations and health

effects of volatile organic compounds (VOCs). Science of the Total Environment, 839, 156201.
Ho, K. F., Lee, S. C., Guo, H., & Tsai, W. Y. (2004). Seasonal and diurnal variations of volatile organic compounds (VOCs) in the atmosphere of Hong Kong. Sci. Total Environ., 322:155–166
https://ww2.arb.ca.gov/sites/default/files/2020-12/cp_reg_mir-tables.pdf
https://www.dpcc.delhigovt.nic.in/
https://environment.delhi.gov.in/
Jain, S., Sharma, S. K., Vijayan, N., & Mandal, T. K. (2020). Seasonal characteristics of aerosols (PM2. 5 and PM10) and their source apportionment using PMF: a four year study over Delhi, India. Environmental Pollution, 262, 114337.
Khoder, M. I. (2007). Ambient levels of volatile organic compounds in the atmosphere of Greater Cairo. Atmospheric Environment, 41(3), 554-566.
Kumar, P., Gurjar, B. R., Nagpure, A. S., & Harrison, R. M. (2011). Preliminary estimates of nanoparticle number emissions from road vehicles in megacity Delhi and associated health impacts. Environmental Science and Technology, 45(13), 5514–5521. https://doi.org/10.1021/es2003183
Krupa S.V., & Manning W. J. (1988). Atmospheric ozone: formation and effects on vegetation. Environmental Pollution. 50(1-2), 101-137. doi: 10.1016/0269-7491(88)90187-x.
Li, Y., Huang, X., Yu, I. T. S., Wong, I. T. S., & Qian, H. (2004). Role of air distribution in SARS transmission during the largest nosocomial outbreak in Hong Kong. Indoor Air, 15, 83-95, PMID: 15737151, DOI: 10.1111/j.1600-0668.2004.00317.x
Li, K., Jacob, D. J., Liao, H., Shen, L., Zhang, Q., & Bates, K. H. (2019). Anthropogenic drivers of 2013–2017 trends in summer surface ozone in China. Proceedings of the National Academy of Sciences of the United States of America, 116(2), 422–427. https://doi.org/10.1073/pnas.1812168116
Li, Y., Liu, B., Ye, J., Jia, T., Khuzestani, R.B., Sun, J.Y., Cheng, X., Zheng, Y., Li, X., Wu, C., Xin, J., Wu, Z., Tomoto, M.A., McKinney, K.A., Martin, S.T., Li, Y.J., & Chen, Q. (2021). Unmanned Aerial vehicle measurements of volatile organic compounds over a subtropical forest in China and implications for emission heterogeneity. ACS Earth Space Chem. 5, 247–56. https://doi.org/10.1021/acsearthspacechem.0c00271
Liu J., Mu, Y., Zhang,Y., Zhang, Z., Wang, X., Liu, Y., & Sun, Z. (2009). Atmospheric levels of BTEX compounds during the 2008 Olympic Games in the urban area of Beijing. Science of the Total Environment, 408(1), 109–116. https://doi.org/10.1016/j.scitotenv.2009.09.026.
Liu, Y. L. Y., Shao, M. S. M., Lu, S. H., Chang, C. C., Wang, J. L., & Fu, L. L. (2008). Source apportionment of ambient volatile organic compounds in the Pearl River Delta, China: Part II. Atmospheric Environment, 42, No. 25, 6261-6274, 10.1016/j.atmosenv.2008.02.027
McDonald, B. C., de Gouw, J. A. , Gilman, J. B. , Jathar, S. H., Akherati, A., Cappa, C. D., Jimenez, J. L., Lee-Taylor, J., Hayes, P. L., McKeen, S. A., Cui, Y. Y., Kim, S.W., Gentner, D. R., Isaacman-VanWertz, G., Goldstein, A. H., Harley, R. A., Frost, G. J., Roberts, J. M., Ryerson, T. B., & Trainer, M. (2018). Volatile chemical products emerging as largest petrochemical source of urban organic emissions. Science, 359(6377), 760-764. doi: 10.1126/science.aaq0524
Miller L., Xu, X., Wheeler, A., Atari, D. O., Mannion, A. G., & Luginaah, I. (2011). Spatial Variability and Application of Ratios between BTEX in Two Canadian Cities, The Scientific World Journal, 11, 2536–2549. ISSN 1537-744X, doi:10.1100/2011/167973
Miller, L., Xu, X., Grgicak-Mannion, A., Brook, J., & Wheeler, A. (2012). Multi-season, multi-year concentrations and correlations amongst the BTEX group of VOCs in an urbanized industrial city. Atmos. Environ., 61:305–315.
Mokalled, T., Le Calvé, S., Badaro-Saliba, N., Abboud, M., Zaarour, R., Farah, W., & Adjizian-Gérard, J. (2018). Identifying the impact of Beirut Airport's activities on local air quality-part I: emissions inventory of NO2 and VOCS. Atmos. Environ. 187, 435–444. https ://doi.org/10.1016/j.atmos env.2018.04.036
Notario, A., Bravo, I., Adame, J. A., Díaz-de-Mera, Y., Aranda, A., Rodríguez, A., & Rodríguez D. (2012). Analysis of NO, NO2, NOx, O3 and oxidant (OX=O3+NO2) levels measured in a metropolitan area in the southwest of Iberian Peninsula. Atmospheric Research, 104–105, 217–226. https://doi.org/10.1016/j.atmosres.2011.10.008

Petrus, M., Popa, C., & Bratu, A. M. (2024). Determination of Ozone Concentration Levels in Urban Environments Using a Laser Spectroscopy System. Environments., 11, 9. https://doi.org/10.3390/environments11010009

Rizwan, S. A., Nongkynrih, B., & Gupta, S. K. (2013). Air pollution in Delhi: Its Magnitude and Effects on Health. Indian Journal of Community Medicine, 38(1), 4–8. https://doi.org/10.4103/0970-0218.106617

Saeedi, M., Malekmohammadi, B., & Tajalli, S. (2024). Interaction of benzene, toluene, ethylbenzene, and xylene with human's body: Insights into characteristics, sources and health risks. Journal of Hazardous Materials Advances, 16, 100459.

Salvador, C. M. G., Alindajao, A. D., Burdeos, K. B., Lavapiez, M. A. M., Yee, J. R., Bautista VII, A. T., Pabroa, P. C. B., & Capangpangan, R. Y. (2022). Assessment of Impact of Meteorology and Precursor in Long-term Trends of PM and Ozone in a Tropical City. Aerosol Air Qual. Res. 22, 210269. https://doi.org/10.4209/aaqr.210269

Schiferl, L. D., Heald, C. L., Nowak, J. B., Holloway, J. S., Neuman, J. A. Bahreini, R. Pollack, I. B., Ryerson, T. B. Wiedinmyer, C., & Murphy J. G. (2014). An investigation of ammonia and inorganic particulate matter in California during the CalNex campaign. J. Geophys. Res. Atmos., 119, 1883–1902. doi:10.1002/2013JD020765.

Seinfeld, J.H., & Pandis, S.N. (2006). Atmospheric Chemistry and Physics: From Air Pollution to Climate Change. 2nd Edition, John Wiley & Sons, New York.

Shi, J, Deng, H, Bai, Z, Kong, S, Wang, X, Hao, J., Han, X., & Ning, P. (2015). Emission and profile characteristic of volatile organic compounds emit-ted from coke production, iron smelt, heating station and power plant in Liaoning Province, China. Sci. Total Environ., 515-516:101–108

Speranza, A., & Rosa, C. (2023). Meteorological variables and PM_{10} exceedances effect on aerosol particles in a low emission zone using compositional data analysis. Journal of Geochemical Exploration, 255, 107322, https://doi.org/10.1016/j.gexplo.2023.107322

Sugimoto, N., Shimizu, A., Matsui, I., & Nishikawa, M. (2016). A method for estimating the fraction of mineral dust in particulate matter using $PM_{2.5}$-to-PM_{10} ratios. Particuology. 28, 114-120, 10.1016/j.partic.2015.09.005

Wang, G., Cheng, S., Wei, W., Zhou, Y., Yao, S., & Zhang, H. (2016). Characteristics and source apportionment of VOCs in the suburban area of Beijing, China. Atmospheric Pollution Research, 7(4), 711-724.

Warneke, C. , Holzinger, R., Hansel A. , Jordan, A. , Lindinger, W. , Pöschl, U. , Williams, J. , Hoor, P. , Fischer, H. , Crutzen, P. J. , Scheeren, H. A. , & Lelieveld, J. (2001). Isoprene and Its Oxidation Products Methyl Vinyl Ketone, Methacrolein, and Isoprene Related Peroxides Measured Online over the Tropical Rain Forest of Surinam in March 1998. Journal of Atmospheric Chemistry, 38(2) DOI: 10.1023/A:1006326802432,

WHO (2016). Report Zika Situation Neurological Sydrom and Congenital Anomalies (Issue February) http://apps.who.int/iris/bitstream/10665/204348/1/zikasitrep_5Feb2016_eng.pdf

Zhang, J., Wei, Y., & Fang, Z. (2019). Ozone Pollution: A Major Health Hazard Worldwide. Front. Immunol. 10, 2518. doi: 10.3389/fimmu.2019.02518